**Atmospheric
Measurement
Techniques**

Profiling tropospheric CO_2 using Aura TES and TCCON instruments

L. Kuai[1], J. Worden[1], S. Kulawik[1], K. Bowman[1], M. Lee[1], S. C. Biraud[2], J. B. Abshire[3], S. C. Wofsy[4], V. Natraj[1], C. Frankenberg[1], D. Wunch[5], B. Connor[6], C. Miller[1], C. Roehl[5], R.-L. Shia[5], and Y. Yung[5]

[1]Jet Propulsion Laboratory, California Institute of Technology, 4800 Oak Grove Drive, Mail stop: 233-200, Pasadena, CA 91109, USA
[2]Lawrence Berkeley National Laboratories, Berkeley, CA 94720, USA
[3]NASA Goddard Space Flight Center, Greenbelt, MD, USA
[4]Harvard University, Cambridge, MA, USA
[5]California Institute of Technology, 1200 E. California Blvd., Pasadena, CA 91125, USA
[6]BC Consulting Ltd., 6 Fairway Dr., Alexandra, 9320, New Zealand

Correspondence to: L. Kuai (lkuai@jpl.nasa.gov)

Abstract. Monitoring the global distribution and long-term variations of CO_2 sources and sinks is required for characterizing the global carbon budget. Total column measurements are useful for estimating regional-scale fluxes; however, model transport remains a significant error source, particularly for quantifying local sources and sinks. To improve the capability of estimating regional fluxes, we estimate lower tropospheric CO_2 concentrations from ground-based near-infrared (NIR) measurements with space-based thermal infrared (TIR) measurements. The NIR measurements are obtained from the Total Carbon Column Observing Network (TCCON) of solar measurements, which provide an estimate of the total CO_2 column amount. Estimates of tropospheric CO_2 that are co-located with TCCON are obtained by assimilating Tropospheric Emission Spectrometer (TES) free tropospheric CO_2 estimates into the GEOS-Chem model. We find that quantifying lower tropospheric CO_2 by subtracting free tropospheric CO_2 estimates from total column estimates is a linear problem, because the calculated random uncertainties in total column and lower tropospheric estimates are consistent with actual uncertainties as compared to aircraft data. For the total column estimates, the random uncertainty is about 0.55 ppm with a bias of -5.66 ppm, consistent with previously published results. After accounting for the total column bias, the bias in the lower tropospheric CO_2 estimates is 0.26 ppm with a precision (one standard deviation) of 1.02 ppm. This precision is sufficient for capturing the winter to summer variability of approximately 12 ppm in the lower troposphere; double the variability of the total column. This work shows that a combination of NIR and TIR measurements can profile CO_2 with the precision and accuracy needed to quantify lower tropospheric CO_2 variability.

1 Introduction

Our ability to infer surface carbon fluxes depends critically on interpreting spatial and temporal variations of atmospheric CO_2 and relating them back to surface fluxes. For example, surface CO_2 fluxes are typically calculated using surface or near-surface CO_2 measurements along with aircraft data (Law and Rayner, 1999; Bousquet et al., 2000; Rayner and O'Brien, 2001; Gurney et al., 2002; Rayner et al., 2008, 2011; Baker et al., 2010; Chevallier et al., 2010, 2011; Keppel-Aleks et al., 2012). More recently it has been shown that total column CO_2 measurements derived from ground-based or satellite observations can be used to place constraints on continental-scale flux estimates (O'Brien and Rayner, 2002; Chevallier, 2007; Chevallier et al., 2011; Keppel-Aleks et al., 2012). However, because CO_2 is a long-lived greenhouse gas, measurements of the total column CO_2 are primarily sensitive to synoptic-scale fluxes (Baker et al.,

2010; Keppel-Aleks et al., 2011); variations in the total column are only partly driven by local surface fluxes, because the total column depends on CO$_2$ from remote locations. Furthermore, the variations caused by the surface source and sinks are largest in the lower tropospheric (LT) CO$_2$ (Sarrat et al., 2007; Keppel-Aleks et al., 2011, 2012). Incorrect specification of the vertical gradient of atmospheric CO$_2$ can also lead to an overestimate of carbon uptake in northern lands and an underestimate of carbon uptake over tropical forests (Stephens et al., 2007). For these reasons we could expect that vertical profile estimates of CO$_2$ will improve constraints on the distributions of carbon flux. Therefore, we are motivated to derive a method to estimate the LT CO$_2$ (surface to 600 hPa) from current available column and free tropospheric (FT) observations.

Total column CO$_2$ data are calculated from solar near-infrared (NIR) measurements from the Total Carbon Column Observing Network (TCCON) (Wunch et al., 2010, 2011a), as well as space-borne instruments, starting from SCIAMACHY (Schneising et al., 2011, 2012) and GOSAT (Yoshida et al., 2009; Wunch et al., 2011b; Crisp et al., 2012; O'Dell et al., 2012). Similar space-borne instruments include OCO-2 (Crisp et al., 2004) and GOSAT-2, which are expected to be launched in 2014 and later this decade respectively. In addition, CarbonSat (Bovensmann et al., 2010; Velazco et al., 2011) is a proposed instrument that could also be launched in the next decade. Ground-based Fourier transfer spectrometer (FTS) measurements such as TCCON instruments have high precision and accuracy compared to satellite instruments but limited spatial coverage. TCCON measurements are therefore a valuable resource for validation of SCIAMACHY, GOSAT and OCO-2 satellite measurements. In addition to the column CO$_2$ from NIR measurements, free tropospheric CO$_2$ measurements can be made from passive thermal infrared satellite instruments such as Tropospheric Emission Spectrometer (TES); (Kulawik et al., 2010, 2012) and AIRS (Chahine et al., 2005). All these measurements by different techniques play important roles in the carbon flux inversion problem and provide complementary information of the atmospheric CO$_2$ distribution. However, none of these instruments measure the LT CO$_2$.

In this paper, we present a method to estimate the LT CO$_2$ by combining column and FT CO$_2$ from two data sources: total column estimates from TCCON and free tropospheric estimates from TES data, assimilated into the GEOS-Chem model. We expect this approach to provide estimates of lower tropospheric CO$_2$, because the TCCON and TES measurements have complementary sensitivities to the vertical distribution of CO$_2$. For example, Fig. 1 shows that TCCON CO$_2$ estimates are sensitive to the total column CO$_2$ as described by its averaging kernel. The averaging kernel indicates the sensitivity of the retrieved estimate to the true distribution of CO$_2$. The TES averaging kernel for an estimate of CO$_2$, averaged from surface to top-of-atmosphere, is also shown in Fig. 1. Both averaging kernels show sensitivity to the free
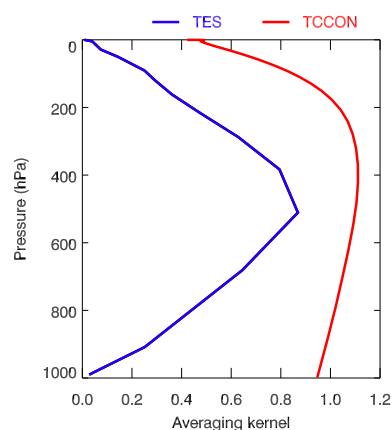

Fig. 1. Averaging kernel for TES retrieval (blue) and TCCON retrieval (red).

tropospheric CO$_2$, whereas the TCCON total column also has sensitivity to the lower tropospheric CO$_2$. Consequently we expect that combining these measurements will allow for estimation of lower tropospheric CO$_2$. This approach has been used to estimate lower tropospheric ozone (Worden et al., 2007; Fu et al., 2012) and carbon monoxide (CO) (Worden et al., 2010). However, we do not use the direct profiling approach discussed in Christi and Stephens (2004), because we found that spectroscopic errors and sampling error due to poor co-location of the NIR and TIR data currently result in unphysical retrieved CO$_2$ profiles. Instead we simply subtract free tropospheric column estimates from total column estimates in order to quantify lower tropospheric CO$_2$ column amounts. As long as the retrievals converge and the estimated states are close to the true states, the problem of subtracting free tropospheric column amount from total column amount is a linear problem with well-characterized uncertainties.
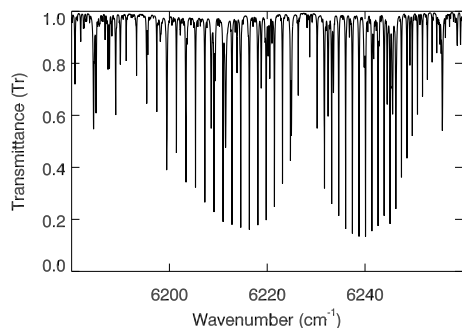
2   Measurements

2.1   Ground-based total column CO$_2$ measurements from TCCON

The column data used to derive LT CO$_2$ in this study are from TCCON observations. These observations are obtained by FTS with a precise solar tracking system, which measures incoming sunlight with high spectral resolution (0.02 cm^{-1}) and high signal-to-noise ratio (SNR) (Washenfelder et al., 2006). The recorded spectra range between 4000–15 000 cm^{-1}. These data provide a long-term observation of column-averaged abundance of greenhouse gases, such as CO$_2$, CH$_4$, N$_2$O and other trace gases (e.g., CO) over 20 TCCON sites around the world, including both operational and future sites (Yang et al., 2002; Washenfelder et al., 2006; Deutscher et al., 2010; Wunch et al., 2010; Messerschmidt et al., 2011). Figure 2 shows a sample measurement

Table 1. Surface fluxes used in GEOS-Chem model.

Biosphere	CASA-GFED3-v2 (3 h) (cmsflux.jpl.nasa.gov)
Biomass burning	GFED3-Fire-v2 (daily) (cmsflux.jpl.nasa.gov)
Bio fuel	GFED3-fuel-v2 (monthly) (cmsflux.jpl.nasa.gov)
Fossil fuel	CDIAC (monthly) (Nassar et al., 2010)
Ocean	ECCO2-Darwin (daily) (cmsflux.jpl.nasa.gov) (Brix et al., 2012)
Ship	ICOADS (monthly) (Nassar et al., 2010)
Chemical source	GEOS-Chem-V8.2.1 (Nassar et al., 2010) (monthly)
Plane emission	GEOS-Chem-V8.2.1 (Nassar et al., 2010) (monthly)
Chemical surface	GEOS-Chem-V8.2.1 (Nassar et al., 2010) (monthly)

Fig. 2. CO_2 band at 1.6 μm observed on 17 June 2008 by TCCON at Park Falls (Wisconsin) with solar zenith angle of 22.5°.

in the 1.6-μm CO_2 absorption band, which is used for analysis here.

As discussed in Wunch et al. (2010, 2011a), total column-averaged abundances can be estimated from TCCON data using a non-linear least squares approach that compares a forward model spectrum against the observed spectrum. The forward model is dependent on CO_2, temperature, water vapor (H_2O), and instrument parameters. The retrieval approach adjusts atmospheric CO_2 concentrations by scaling an a priori CO_2 profile until the observed and modeled spectra agree within the noise levels. The precision in the column-averaged CO_2 dry air mole fraction from the scaling retrievals is better than 0.25 % (Wunch et al., 2010, 2011a). The absolute accuracy is $\sim$ 1 %; after calibration by aircraft data, the absolute accuracy can reach 0.25 % (Wunch et al., 2010, 2011a).

In this paper, we use the optimal estimation method (Rodgers, 2000) to retrieve a profile that scales multiple levels of the CO_2 profile instead of the whole profile (Kuai et al., 2012). We find that the precision of retrieved column averages of the profile using this approach (0.55 ppm) is consistent with the scaling retrievals described by Wunch et al. (2010). The profile retrieval algorithm is described in Sect. 4.

2.2 Satellite-based free tropospheric CO_2 measurements from TES

Free tropospheric CO_2 estimates are derived from thermal IR radiances measured by the Tropospheric Emission Spectrometer (TES) aboard NASA's Aura satellite (Beer et al., 2001). The TES instrument measures the infrared radiance emitted by Earth's surface and atmospheric gases and particles from space. These measurements have peak sensitivity to the mid-tropospheric CO_2 at $\sim$ 500 hPa (Kulawik et al., 2012). The sampling for the TES CO_2 measurements is sparse (e.g., 1 measurement every 100 km approximately), and the satellite passes over the Lamont TCCON site $\sim$ every 16 days (Beer et al., 2001). However, the spatial scales of variability in the free troposphere are large, which suggests that TES data can provide useful constraints on free tropospheric CO_2 over TCCON sites. In order to exploit these large scales, we assimilated the TES CO_2 measurements into the GEOS-Chem model, a global 3-D chemistry transport model (CTM).

GEOS-Chem (V8.2.1) is driven by assimilated meteorological data from the Goddard Earth Observation System (GEOS) of the NASA Global Modeling and Assimilation Office (GMAO). The model supports input data from GEOS-4 (1° × 1.25° horizontal resolution, 55 vertical levels), GEOS-5 (0.5° × 0.67°, 72 levels), and MERRA (ibid.). The GEOS meteorological data archive has a temporal resolution of 6 h except for surface quantities and mixing depths that have temporal resolution of 3° × 2.5° or 4° × 5° grid resolution by aggregating GEOS meteorological data (Bey et al., 2001). Convective transport in GEOS-Chem is computed from the convective mass fluxes in the meteorological archive, as described by Wu et al. (2007) for GEOS-4, GEOS-5, and GISS GCM 3.

The original CO_2 simulation in GEOS-Chem was described by Suntharalingam et al. (2004) and was updated by Nassar et al. (2010). The "bottom-up" inventories used to force GEOS-Chem are drawn from Nassar et al. (2010) and from the Carbon Monitoring System Flux Pilot Project (http://carbon.nasa.gov) and are available at http://cmsflux.jpl.nasa.gov. The specific inventories are described in Table 1. TES CO_2 and flask measurements have been used to

constrain time-invariant global carbon fluxes in GEOS-Chem (Nassar et al., 2011). Both 3-D variational (3-D var) and 4-D variational (4-D var) assimilation approaches have been implemented in GEOS-Chem for full oxidant-aerosol chemistry as well as for CO (Henze et al., 2007, 2009; Kopacz et al., 2009; Singh et al., 2011a,b). These techniques have been used to assess the impact of precursors and emissions on atmospheric composition (Zhang et al., 2009; Walker et al., 2012; Parrington et al., 2012). The 3-D var assimilation algorithm used here is adapted from Singh et al. (2011b).

TES at all pressure levels between 40° S–40° N, along with the predicted sensitivity and errors, was assimilated for the year 2009 using 3-D var assimilation. We compare model output with and without assimilation to surface-based in situ aircraft measurements from the US DOE Atmospheric Radiation Measurement (ARM) Southern Great Plains (SGP) site during the ARM Airborne Carbon Measurements (Biraud et al., 2012, http://www.arm.gov/campaigns/aaf2008acme) and HIAPER Pole-to-Pole Observations-II (HIPPO-2; http://hippo.ucar.edu/) campaigns (Kulawik et al., 2012). We find model improvement in the seasonal cycle amplitude in the mid-troposphere at the SGP site, but there are model discrepancies compared with HIPPO at remote oceanic sites, particularly outside of the latitude range of assimilation (Kulawik et al., 2012).

We use the results from the assimilation as our estimates of free tropospheric CO_2. The uncertainties in the assimilation fields are calculated as the difference from aircraft data (Sect. 5.2).

2.3 Flight measurements

Aircraft data are used as our standard to assess the quality of the different CO_2 estimates. The aircraft measure CO_2 profiles typically up to 6 km and sometimes to 10 km or higher. For comparison with the TCCON CO_2 estimates, we collected profile observations from different aircraft campaigns, such as HIPPO (Wofsy et al., 2011) and Learjet (Abshire et al., 2010) (http://www.esrl.noaa.gov/gmd/ccgg/aircraft/qc.html), and ARM-SGP (Biraud et al., 2012) (http://www.arm.gov/campaigns/aaf2008acme) over the year 2009. These data are compared to the TCCON CO_2 observations at the Lamont site, Oklahoma (36.6° N, 97.5° W).

3 Calculation of total column and LT CO_2

Our approach is to estimate LT CO_2 by subtracting estimates of partial column CO_2 in the free troposphere from the total column CO_2. The total column of a gas "g", denoted by C_g, is obtained by integrating the gas concentration profile from the surface to the top of atmosphere:

$$C_g = \int_0^{\propto (p=0)} f_g^{\text{dry}}(z) \cdot n_{\text{dry}}(z) \cdot \mathrm{d}z \qquad (1)$$

where $f_g^{\text{dry}}(z)$ and $n_{\text{dry}}(z)$ are the vertical profiles of the dry-air gas volume mixing ratio and number density, respectively, as functions of altitude z. The dry-air column-averaged mole fraction of CO_2, denoted by X_{CO_2}, is defined as the ratio of the total dry-air column of CO_2 to that of dry air:

$$X_{CO_2} = \frac{C_{CO_2}}{C_{\text{air}}} \qquad (2)$$

where C_{CO_2} and C_{air} are obtained by Eq. (1).

In real atmosphere where the amount of H_2O cannot be neglected, $f_g^{\text{dry}}(z)$ is formally defined as

$$f_g^{\text{dry}}(z) = \frac{f_g(z)}{1 - f_{H_2O}(z)}. \qquad (3)$$

However, the H_2O concentration is usually highly variable and may introduce some uncertainties in $f_g^{\text{dry}}(z)$. On the other hand, TCCON also provides precise measurements of O_2. Dividing by the retrieved O_2 using spectral measurements from the same instrument improves the precision of X_{CO_2} by significantly reducing the effects of instrumental/measurement errors that are common in both gases (e.g., solar tracker pointing errors, zero level offsets, instrument line shape errors, etc.) (Wunch et al., 2010). Therefore, we introduce another definition of $f_g^{\text{dry}}(z)$ by normalizing simultaneously retrieved O_2:

$$f_g^{\text{dry}}(z) = \frac{f_g(z)}{f_{O_2}(z)} \times 0.2095. \qquad (4)$$

Consistent with the discussions in Wunch et al. (2010), the precision of column estimates using O_2 as the dry air standard will be improved, but the bias specific from the use of the O_2 band will be transferred to X_{CO_2}. For example, Fig. 3 shows total column X_{CO_2} estimates, retrieved from our algorithm, corresponding to aircraft in which data were taken from the surface past 10 km. Red points represent X_{CO_2}, which is estimated using Eq. (3); black points represent X_{CO_2}, which is estimated using Eq. (4). Dots are used for Park Falls site, and diamonds are applied for Lamont site.

As evident from Fig. 3, X_{CO_2} estimated using Eq. (4) with the observed O_2 column has higher precision, but it also has $\sim 1\%$ negative bias (Wunch et al., 2010, 2011a). Because the bias is relatively constant over time and over different sites as discussed in Wunch et al. (2010), we remove this mean bias in TCCON X_{CO_2} when estimating the total column amount:

$$C_{CO_2} = C_{\text{air}} \left(\frac{X_{CO_2}^{\text{TCCON}}}{\alpha} \right) \qquad (5)$$

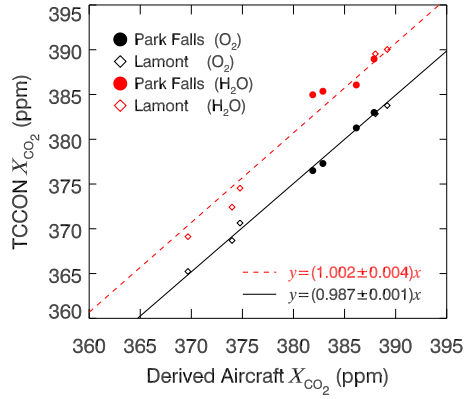where α is an empirical correction factor to remove the bias in TCCON column retrievals.

Fig. 3. Comparison of X_{CO_2} estimates to derived aircraft column averages. Red points indicate that H_2O is used as dry air standard. Black points indicate that O_2 is used as dry air standard. Dots are for Park Falls site and diamonds for Lamont site. Error bars are not shown in this figure.

The partial vertical column amount of CO_2 in free troposphere and above ($C_{CO_2}^{TROP}$) is estimated by integrating the TES/GEOS-Chem assimilated profile ($f_{CO_2}^{TES}$) above 600 hPa.

$$C_{CO_2}^{TROP} = \int_{z(p=600)}^{\propto(p=0)} f_{CO_2}^{TES}(z) \cdot n_{dry}(z) \cdot dz. \quad (6)$$

The partial vertical column amount of CO_2 in the LT can then be computed as the difference between the total column amount (Eq. 6) and partial free tropospheric column amount (Eq. 7):

$$C_{CO_2}^{LT} = C_{air} \left(\frac{X_{CO_2}^{TCCON}}{\alpha} \right) - \int_{z(p=600)}^{\propto(p=0)} f_{CO_2}^{TES}(z) \cdot n_{dry}(z) \cdot dz. \quad (7)$$

Applying Eq. (3) within the lower troposphere gives the estimate of the LT CO_2 mole fraction ($X_{CO_2}^{LT}$); the ratio of partial vertical column between CO_2 ($C_{CO_2}^{LT}$) and air ($C_{air}^{LT} = \int_{0}^{z(p=600)} 1 \cdot n_{dry}(z) \cdot dz$) is

$$X_{CO_2}^{LT} = \frac{\frac{X_{CO_2}^{TCCON}}{\alpha} \int_{0}^{\propto(p=0)} 1 \cdot n_{dry}(z) \cdot dz - \int_{z(p=600)}^{\propto(p=0)} f_{CO_2}^{TES}(z) \cdot n_{dry}(z) \cdot dz}{\int_{p_s}^{600} 1 \cdot n_{dry}(z) \cdot dz} \quad (8)$$

where $X_{CO_2}^{LT}$ is defined as the TCCON/TES LT CO_2. These estimates can be compared to the integrated partial column-averaged CO_2 measured by aircraft within the lower troposphere (surface to 600 hPa for Lamont).

4 CO_2 profile retrieval approach

In this section, we describe a profile retrieval algorithm that is based on the scaling retrieval discussed in Wunch et al. (2010, 2011a). Characterization of the errors, based on this retrieval approach, is discussed in the Appendix. The profile of atmospheric CO_2 is obtained by optimal estimation (Rodgers, 2000) using the same line-by-line radiative transfer model discussed in Wunch et al. (2010) (or the standard TCCON retrieval algorithm: GFIT). It computes simulated spectra using 71 vertical levels with 1 km intervals for the input atmospheric state (e.g., CO_2, H_2O, HDO, CH_4, O_2, P, T, etc.). The details about the TCCON instrument setup and GFIT are also described in Yang et al. (2002), Washenfelder et al. (2006), Deutscher et al. (2010), Geibel et al. (2010) and Wunch et al. (2010, 2011a). The retrievals in this study use one of TCCON-measured CO_2 absorption bands, centered at 6220.00 cm^{-1} with a window width of 80.00 cm^{-1} (Fig. 2). Note that ultimately we do not use the full profiles for this study as we find that spectroscopic or other errors introduce vertical oscillations into the estimated profiles with larger values than expected in the upper troposphere that are compensated by lower values than expected in the lower troposphere. The same effect is found in the GOSAT CO_2 retrievals as discussed in O'Dell et al. (2012). This vertical oscillation is one of the potential issues in joint retrievals by combining NIR and TIR (thermal infrared) radiance in addition to the limitation of the coincident measurements from two different instruments. However, the total columns of these profiles are still good estimates with well-characterized errors as discussed in Sect. 5.1. Therefore, the profiles are mapped into column amounts and are shown to be consistent with the results of Wunch et al. (2011a). We use a profile retrieval instead of standard TCCON column scaling retrieval in order to understand the error characteristics of the CO_2 retrieval.

In the scaling retrieval discussed by Wunch et al. (2010, 2011a), the retrieved state vector (γ) includes the eight constant scaling factors for four absorption gases (CO_2, H_2O, HDO, and CH_4) and four instrument parameters (continuum level: "cl", continuum tilt: "ct", frequency shift: "fs", and zero level offset: "zo").

$$\gamma = \begin{bmatrix} \gamma_{[CO_2]} \\ \gamma_{[H_2O]} \\ \gamma_{[HDO]} \\ \gamma_{[CH_4]} \\ \gamma_{cl} \\ \gamma_{ct} \\ \gamma_{fs} \\ \gamma_{zo} \end{bmatrix} \quad (9)$$

Each element of γ is a ratio between the state vector (x) and its a priori (x_a). In the profile retrieval, for the target gas
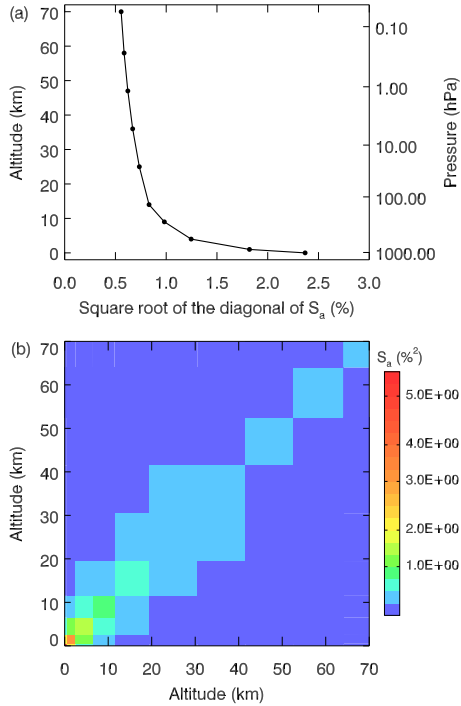
Fig. 4. (a) The square root of the diagonal in CO$_2$ covariance matrix. **(b)** The 2-D plot of the CO$_2$ covariance matrix.

(CO$_2$), we estimate the altitude-dependent scaling factors instead. For other interfering gases, a single scaling factor is retrieved. Ten levels are chosen for CO$_2$ (see Fig. 4a) to capture its vertical variation:

$$\boldsymbol{\gamma} = \begin{bmatrix} \gamma_{1[CO_2]} \\ \vdots \\ \gamma_{10[CO_2]} \\ \gamma_{[H_2O]} \\ \gamma_{[HDO]} \\ \gamma_{[CH_4]} \\ \gamma_{cl} \\ \gamma_{ct} \\ \gamma_{fs} \\ \gamma_{zo} \end{bmatrix}. \tag{10}$$

To obtain a profile of volume mixing ratio, the retrieved scaling factors need to be mapped from retrieval grid (i.e., 10 levels for CO$_2$ and 1 level for other three gases) to the 71 forward model levels.

$$\boldsymbol{\beta} = \mathbf{M}\boldsymbol{\gamma} \tag{11}$$

where $\mathbf{M} = \frac{\partial \beta}{\partial \gamma}$ is a linear mapping matrix relating retrieval level to the forward model altitude grid. Multiplying the scaling factor ($\boldsymbol{\beta}$) on the forward model level to $\mathbf{M}_x = \frac{\partial x}{\partial \beta}$, a diagonal matrix of the concentration a priori ($\boldsymbol{x}_a$), gives the true state of gas profile:

$$\boldsymbol{x} = \mathbf{M}_x \boldsymbol{\beta}. \tag{12}$$

According to the above definition, the a priori profile is $\boldsymbol{x}_a = \mathbf{M}_x \beta_a$ and estimated state is $\hat{\boldsymbol{x}} = \mathbf{M}_x \hat{\beta}$.

The non-linear least squares retrieval is a standard optimal estimation retrieval that employs an a priori constraint matrix to regularize the problem (Rodgers, 2000; Bowman et al., 2006). The non-diagonal CO$_2$ covariance matrix used to generate the constraint matrix has larger variance in the lower troposphere and decreases with altitude. This covariance is generated using the GEOS-Chem model as guidance. However, we scale the diagonals of the covariance matrix in order to match the variability observed at the TCCON sites. The square root of the diagonal of this covariance is approximately 2 % (8 ppm) in the lower troposphere, 1 % (4 ppm) in the free troposphere, and less than 1 % (4 ppm) in the stratosphere (Fig. 4a). The off-diagonal correlations are shown in Fig. 4b. The elements of the a priori covariance corresponding to the other retrieved parameters (e.g., H$_2$O) are set to be equivalent to 100 % uncertainty.

The measurement noise, or signal-to-noise ratio (SNR) is used to weight the measurement relative to the a priori in the non-linear least squares retrieval. Although the SNR of the TCCON instrument is better than 500, we use a SNR of approximately 200, because spectroscopic uncertainties degrade the comparison (O'Dell et al., 2011; Wunch et al., 2011a); use of this SNR results in a *chi-square* in our retrievals of about 1.

To obtain the best estimate of the state vector that minimizes the difference between the observed spectral radiances (y_o) and the forward model spectral radiances (y_m), we perform Bayesian optimization by minimizing the cost function, $\chi(\boldsymbol{\gamma})$:

$$\chi(\boldsymbol{\gamma}) = (y_m - y_o)^T \mathbf{S}_e^{-1}(y_m - y_o) + (\boldsymbol{\gamma} - \boldsymbol{\gamma}_a)^T \mathbf{S}_a^{-1}(\boldsymbol{\gamma} - \boldsymbol{\gamma}_a) \tag{13}$$

where $\mathbf{S}_a$ is chosen to be the covariance shown in Fig. 4 and $\mathbf{S}_e$ is the measurement noise covariance, a diagonal matrix with values of noise squared. Noise is inverse of SNR.

5 Results

5.1 Quality of the column-averaged CO$_2$ estimates

To characterize the quality of the CO$_2$ estimates, we compare the TCCON column-averaged estimates with the aircraft column-integrated data. Calculated errors (as derived in the Appendix) are compared to actual errors as derived empirically from comparison of the estimates to the aircraft data and are shown to be consistent.

There are 41 SGP aircraft-measured CO$_2$ profiles in 2009 (Fig. 5). Most aircraft measurements are from the surface to 6 km; however, three profiles have measurements from the surface to 10 km or higher (31 July, 2 and 3 August). To estimate the total column, the CO$_2$ values for altitudes above the top of the aircraft measurements are replaced by the TCCON CO$_2$ a priori, shifted to match the mean aircraft value
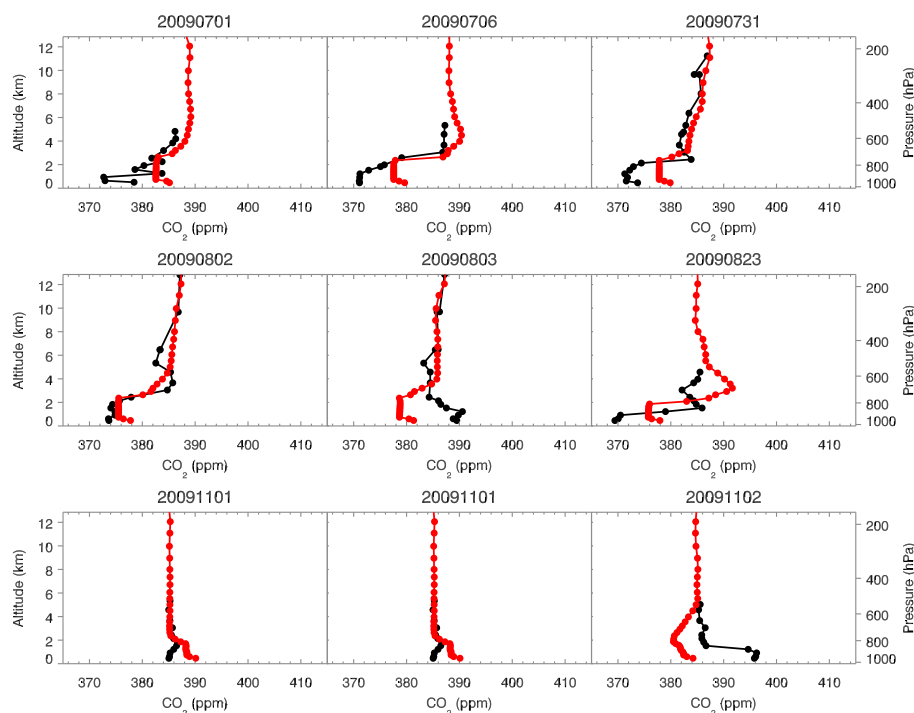
Fig. 5. Samples of CO_2 profiles measured by aircraft (black) and TES/GEOS-Chem assimilation (red) at SGP.

at the top of the aircraft profile. As discussed in the Appendix (A1.2.1), this approximation to the upper tropospheric CO_2 values negligibly contributes to uncertainty in the comparison between TCCON X_{CO_2} estimates and the aircraft + shifted upper troposphere a priori profiles. The comparisons between TCCON column averages and the derived aircraft column averages are summarized in Fig. 6 and Table 2.

TCCON X_{CO_2} estimates are calculated within a 4-h time window, centered about the time corresponding to each aircraft profile. A 4-h time window is chosen to ensure that comparisons are statistically meaningful and also to ensure that variations in CO_2 and temperature are small relative to calculated uncertainties. Comparisons between TCCON and aircraft X_{CO_2} are shown in Table 2. Results listed in Table 2 are only for clear-sky scenes, because it is difficult to quantify the effect of clouds on the TCCON retrievals and errors. We find that the calculated precision for the collection of measurements within each 4-h time window encompassing the aircraft is, on average, approximately 0.32 ppm. This precision is, on average, consistent with the variability of the TCCON X_{CO_2} estimates within this 4-h time window of 0.35 ppm. The error on the mean will be arbitrarily small because of the large number of measurements within this 4-h time window. Consequently, we expect that the X_{CO_2} variability within each 4-h time window is driven by noise and not by variations in temperature and CO_2. However, we calculate that errors in temperature lead to an error in X_{CO_2} of approximately 0.69 ppm on average (last column, Table 2). We find that the TCCON X_{CO_2} estimates are biased on
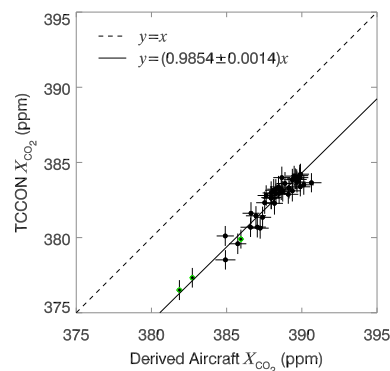

Fig. 6. Comparison of X_{CO_2} from TCCON profile retrievals to that derived from aircraft. Black dots indicate comparison of TCCON estimates to aircraft that measure up to 6 km. Green dots are comparison of TCCON estimates to the three aircraft profiles that measure up to 12 km.

average by -5.66 ± 0.55 ppm. The magnitude of this bias estimate is consistent with that described in Wunch et al. (2010) and is attributed to errors in the O_2 spectroscopy. The error in the bias (0.55 ppm) is consistent with the calculated error due to temperature (0.69 ppm) and is a result of temperature variations between aircraft measurements.

Table 2. Lists of bias error and its standard deviation ($1 \times \sigma$) of TCCON profile retrieved column averages within 4-h time window of each flight measurement. The expected uncertainties from measurement error covariance and the temperature error covariance are also listed in the last two columns. To remove the unclear sky spectra measurements, we dismiss the retrievals when the parameter "fvis" (fractional variation in solar intensity) is greater than 0.05, which suggests the cloud coverage during the spectra measurement. By applying the cloud filter, the consistency between the empirical error estimates and expected error estimates is improved. The columns for "n" are the total numbers of retrievals within 4-h time window.

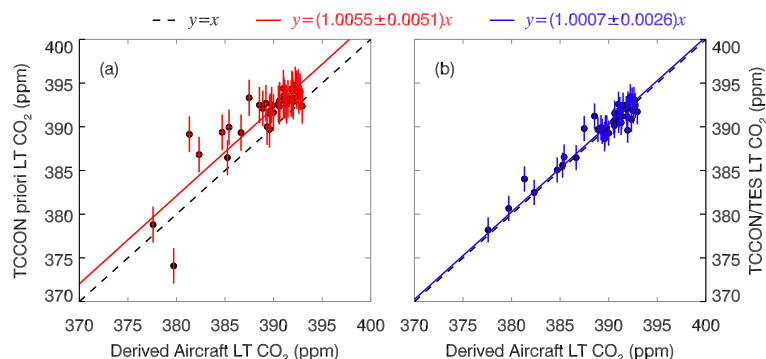| Unit (ppm)	With cloud filter			Expected	
Day (yyyymmdd)	Bias + 5.66 (ppm)	Actual ($1 \times \sigma$)	n	$\sigma\left(\delta X_{CO_2}^{h}\right)$	$\sigma\left(\delta X_{CO_2}^{day}\right)$
20090108	0.66	0.30	161	0.27	0.74
20090116	0.45	0.30	171	0.33	0.74
20090129	0.36	0.30	169	0.34	0.77
20090204	0.58	0.26	169	0.33	0.74
20090211	0.69	0.49	90	0.33	0.75
20090219	0.39	0.38	96	0.33	0.76
20090221	0.67	0.42	130	0.34	0.77
20090308	0.25	0.39	132	0.32	0.71
20090314	0.98	0.42	102	0.33	0.73
20090316	0.00	0.27	154	0.32	0.69
20090318	0.26	0.44	112	0.32	0.69
20090329	−0.08	0.28	76	0.33	0.72
20090407	0.13	0.26	98	0.33	0.72
20090408	−0.03	0.40	121	0.32	0.69
20090420	−0.59	0.44	69	0.32	0.70
20090421	−0.32	0.29	130	0.32	0.70
20090423	−0.21	0.30	122	0.32	0.66
20090517	−0.19	0.32	130	0.32	0.70
20090518	0.82	0.32	131	0.32	0.68
20090520	0.60	0.50	75	0.32	0.67
20090526	−0.12	0.36	86	0.32	0.67
20090528	0.11	0.30	130	0.32	0.68
20090530	0.30	0.34	130	0.32	0.66
20090604	0.01	0.38	128	0.32	0.68
20090612	−0.96	0.35	72	0.32	0.66
20090616	−1.31	0.34	128	0.31	0.64
20090621	−0.85	0.28	95	0.31	0.63
20090623	−0.56	0.32	129	0.31	0.63
20090629	0.16	0.32	118	0.31	0.64
20090701	−0.24	0.46	119	0.31	0.65
20090706	0.85	0.33	43	0.32	0.66
20090731	0.31	0.34	125	0.32	0.66
20090802	0.26	0.29	131	0.31	0.65
20090803	−0.37	0.33	130	0.31	0.63
20090823	−0.74	0.38	130	0.31	0.65
20091101	−0.47	0.36	130	0.32	0.68
20091102	−0.68	0.33	131	0.32	0.69
20091103	−0.94	0.35	131	0.32	0.70
20091122	−0.38	0.39	68	0.32	0.71
20091218	−0.23	0.47	127	0.33	0.75
20091220	0.33	0.38	101	0.33	0.72
Mean	0.00	0.35	118	0.32	0.69
$1 \times \sigma$	0.55				

Fig. 7. (a) Comparison of LT CO_2 estimates derived from integrating from surface to 600 hPa by TCCON prior and aircraft. **(b)** Comparison of LT CO_2 estimates derived from TCCON and TES with aircraft.

5.2 Quality of the LT CO_2 estimates

In this section we examine the robustness of estimates of the LT CO_2 (surface to 600 hPa) by comparison of the TC-CON/TES LT CO_2 to aircraft estimates. We separate the lower troposphere from the free troposphere at the 600 hPa pressure level, because the aircraft profiles indicate that the variability in the free troposphere becomes "small" above this pressure (Fig. 5) relative to the variability below this level and it is well above the boundary layer height, which varies depending on the location and time of the day. The knowledge of the boundary layer height will affect the use of these LT estimates for quantifying surface fluxes, because boundary layer heights are typically at higher pressures than 600 hPa (von Engeln et al., 2005). Figure 7a compares the LT CO_2 estimates that are calculated from integrating TC-CON prior from surface to 600 hPa to the aircraft estimates. Figure 7b compares the LT CO_2 estimates that are calculated from TCCON and TES data to the aircraft estimates. The root-mean-square (RMS) of the fitted line (1.02 ppm) in Fig. 7b is smaller than that if the TCCON prior data are used in Fig. 7a (2.02 ppm). The -5.66 ppm bias (or factor α in Eq. 9) is removed from the TCCON total column before computing the LT CO_2 using TCCON data and TES data. As shown in Table 3, the average difference between TC-CON/TES LT CO_2 and aircraft values is 0.26 ± 1.02 ppm. The calculated uncertainty (Appendix A4, Eq. A28) depends on the quadratic sum of the uncertainties of TES free tropospheric estimates (~ 0.71 ppm) and TCCON column estimates (~ 0.55), resulting in an estimate of uncertainty of 0.90 ppm. This calculated uncertainty of 0.90 ppm is consistent with the actual uncertainty of 1.02 ppm. For total column CO_2, the retrieved value from TCCON measurement is a better estimate than TCCON prior. For free tropospheric CO_2, the assimilated value from TES/GEOS-Chem has the smallest uncertainty (0.71 ppm) and is thus a better estimate compared to the other estimates (e.g., TCCON prior, TCCON retrieval, or GEOS-Chem modeling). As a result, for LT CO_2, the retrieved value from the TCCON/TES retrieval is the best

Table 3. Bias and precision comparisons.

Unit (ppm)		Bias	Precision
Total column CO_2	[TCCON prior]	1.04	1.50
	[TCCON]	-5.66	0.55
FT CO_2	[TCCON prior]	0.23	1.33
(Above 600 hPa)	[TCCON]	-1.62	1.50
	[GEOS-Chem]	0.91	1.22
	[TES/GEOS-Chem]	0.38	0.71
LT CO_2	[TCCON prior]	2.17	2.05
(Surface to 600 hPa)	[TCCON]	-4.91	1.39
	[GEOS-Chem]	0.13	1.92
	[TES/GEOS-Chem]	0.73	2.86
	[TCCON] $-$ [TES/GEOS-Chem]	0.26	1.02

estimate compared to the TCCON priori, GEOS-Chem modeling and TES/GEOS-Chem assimilation. In addition, the improvement in the TCCON/TES LT CO_2 (1.02 ppm), relative to the TCCON priori (2.0 ppm), is mainly during summertime when surface CO_2 is low relative to wintertime, because the biosphere is more active in the summer (Fig. 7). With these uncertainties, the LT CO_2 estimates are able to capture the seasonal variability of the lower troposphere as discussed next.

5.3 Seasonal variability of LT CO_2 compared to column CO_2

The aircraft, TCCON, and TES assimilated estimates of atmospheric CO_2 have sufficient temporal density to provide an estimate of CO_2 variability over most of the year. In Fig. 8 we show the monthly averaged total column averages and the partial column averages (surface to 600 hPa) calculated from the aircraft data and the same quantities derived from the TCCON data and the TCCON minus TES assimilated data respectively. The TCCON column averages (black dots) and TCCON/TES derived LT data (red dots) are consistent with the aircraft measurement (black diamonds and red diamonds) within the expected uncertainties indicating that the estimates are robust. We use a total of 41 aircraft profiles.
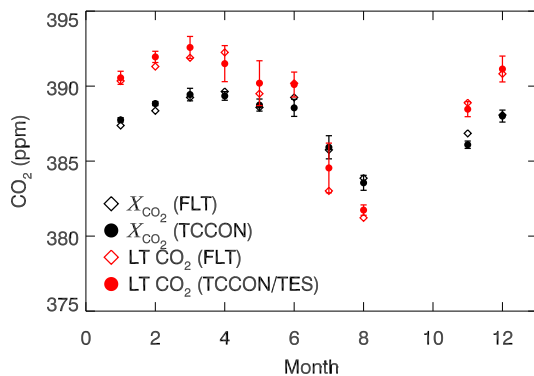
Fig. 8. Monthly mean X_{CO_2} for total column and LT CO_2 in 2009 at Lamont. Aircraft data (FLT) are indicated by diamonds (black for total X_{CO_2}; red for LT CO_2) and TCCON or TCCON/TES estimates are indicated by black or red dots with error bars.

Typically 3–5 profiles have been averaged in a month. However, September and October both have only one available aircraft profile, which were measured under cloudy skies. So September and October data cannot be used in this study. Therefore, the comparisons for these two months are not shown. In Fig. 8, both TCCON column averages and TCCON/TES LT CO_2 capture the seasonal variability.

The response of the seasonal variability in LT CO_2 is more than twice that of the column averages with a 14-ppm peak-to-trough in LT CO_2 and 5 ppm in the column-averaged CO_2. This increased variability is due to a rapid drawdown in LT CO_2 at the growing season onset over mid-latitude due to the biosphere uptake.

6   Summary

Total column estimates of atmospheric CO_2 and partial column estimates of CO_2 in the lower troposphere (surface to 600 hPa) are calculated using TCCON and Aura TES data. In order to determine if the retrieval approach, forward model, and understanding of uncertainties are robust, it is crucial to determine if the calculated uncertainties are consistent with the actual uncertainties. In addition, we need to assess any biases in the estimates and ideally attribute these bias errors in the measurement system. The bias and its uncertainties in TCCON column-averaged CO_2 are explained at two different time scales: 4-h time windows centered about individual aircraft measurement and day-to-day time scales from comparison to the collection of 41 aircraft profiles. We find that, for multiple retrievals of the same air parcel within a 4-h time window, the mean bias is from the uncertainties of atmospheric states (i.e., temperature or interference gases) or spectroscopic parameters. The variability of the collection of total column estimates within the 4-h time window of 0.35 ppm is consistent with the calculated random error of about 0.32 ppm, which is associated with

the measurement error. When comparing the TCCON total column estimates to aircraft data over several days, we can assume that the daily systematic errors due to temperature or other interference error are pseudo-random. For example, the estimated mean bias across multiple days is -5.66 (± 0.55) ppm. The standard deviation of the bias error of approximately 0.55 ppm is consistent with the expected error of 0.69 ppm, which is primarily driven by temperature error, because measurement error for these comparisons is arbitrarily small due to the large number of measurements used to calculate the mean CO_2 estimate.

Comparisons of the aircraft data to free tropospheric CO_2, calculated by assimilating Aura TES CO_2 estimates into the GEOS-Chem model (Nassar et al., 2011), suggest that the TES assimilated data have a bias error of 0.38 (± 0.71) ppm in the free troposphere. We calculated a lower tropospheric estimate (surface to 600 hPa) of the CO_2 amount by subtracting the TES assimilated free tropospheric estimate from the TCCON total column amount estimates. Comparisons of these lower tropospheric estimates from TCCON/TES data to those from aircraft data are consistent after the bias in the TCCON is removed. The precision in the derived LT CO_2 is 1.02 ppm, which is consistent with the calculated precision of 0.90 ppm. The dominant sources of the error in the LT estimates are due to uncertainties in the free troposphere data from TES assimilation and the temperature-driven error in column averages from TCCON. We show that this precision is sufficient to characterize the seasonal variability of lower tropospheric CO_2 over the Lamont TCCON site.

The approach described in this paper shows that the problem of using independent total column and free tropospheric estimates to estimate lower tropospheric CO_2 is a linear problem. This linear problem is in contrast to using a non-linear retrieval for quantifying lower tropospheric ozone (Worden et al., 2007) or CO (Worden et al., 2010) by using reflected sunlight and thermal IR radiances and is likely, because ozone and CO can have much larger variance in the lower troposphere than CO_2.

The study shown here indicates that assimilating total column and free tropospheric CO_2 will increase sensitivity to surface fluxes by placing improved constraints on lower tropospheric CO_2. Furthermore, quantifying lower tropospheric CO_2 using total column and free tropospheric estimates is useful for evaluating model estimates of lower troposphere.

This study also highlights the potential of combining simultaneous measurements from NIR and IR sounding instruments to obtain vertical information of atmospheric CO_2 (Christi and Stephens, 2004). Column estimates of CO_2 by space are currently available from GOSAT (Yoshida et al., 2009) and SCIAMACHY data (Schneising et al., 2011, 2012) and are expected from OCO-2. Column CO_2 estimates from these satellite data together with the free tropospheric CO_2 estimates are anticipated to provide complementary constraints to infer CO_2 fluxes and advance the ability to study the carbon cycle problem by providing constraints

on near-surface CO_2 variations and atmospheric mixing. Our future work will apply this method to combine GOSAT and TES data to expand the spatial coverage of these lower tropospheric CO_2 estimates.

Appendix A

Error characterization

One of the reasons we used optimal estimation to retrieve the CO_2 profile and then map the profile to the total column CO_2 instead of using the standard TCCON product is that the optimal estimation allows us to characterize the error budget. This appendix estimates the expected errors and shows how these terms compare to the actual errors. Careful characterization of the errors is critical for evaluating the retrieval mechanics and for use of these data for scientific analysis.

A1 Errors in TCCON column-averaged CO_2

In this section, we develop the error characterization for (1) the estimates of TCCON CO_2 column averages from the profile retrievals for a 4-h time window around each aircraft CO_2 profile measurement and (2) comparisons of TCCON estimates against 41 aircraft profiles.

In addition to CO_2, we also retrieve a column amount of H_2O, HDO and four instrument parameters. This set of retrieval parameters is defined in the following retrieval vector (see Sect. 4):

$$\boldsymbol{\gamma} = \begin{bmatrix} \gamma_{1[CO_2]} \\ \vdots \\ \gamma_{10[CO_2]} \\ \gamma_{[H_2O]} \\ \gamma_{[HDO]} \\ \gamma_{[CH_4]} \\ \gamma_{cl} \\ \gamma_{ct} \\ \gamma_{fs} \\ \gamma_{zo} \end{bmatrix}. \tag{A1}$$

Each element of $\boldsymbol{\gamma}$ is a ratio between the state vector ($\boldsymbol{x}$) and its a priori ($\boldsymbol{x}_a$). For the target gas CO_2, altitude-dependent scaling factors are retrieved. For other interfering gases, a constant scaling factor for the whole profile is retrieved. The last four are for the instrument parameters (continuum level: "cl", continuum title: "ct", frequency shift: "fs", and zero level offset: "zo"). To obtain a concentration profile, the retrieved scaling factors are mapped from the retrieval grid (i.e., 10 levels for CO_2 and 1 level for other three gases) to the 71 forward model levels.

$$\beta = \mathbf{M}\boldsymbol{\gamma} \tag{A2}$$

where $\mathbf{M} = \frac{\partial \beta}{\partial \gamma}$ is a linear mapping matrix relating retrieval levels to the forward model altitude grid. Multiplying the

scaling factor (β) on the forward model level to the concentration a priori ($\boldsymbol{x}_a$) gives the estimates of the gas profile. We define $\mathbf{M}_x = \frac{\partial x}{\partial \beta}$ where $\mathbf{M}_x$ is a diagonal matrix filled by the concentration a priori ($\boldsymbol{x}_a$):

$$\hat{\boldsymbol{x}} = \mathbf{M}_x \hat{\beta}. \tag{A3}$$

From Eq. (A3), it follows that $\boldsymbol{x}_a = \mathbf{M}_x \beta_a$ and $\boldsymbol{x} = \mathbf{M}_x \beta$. The Jacobian matrix of retrieved parameter with respect to the radiance is

$$\mathbf{K}_\gamma = \frac{\partial \mathbf{L}(\mathbf{M}\boldsymbol{\gamma})}{\partial \boldsymbol{\gamma}}. \tag{A4}$$

Using the chain rule, we can obtain the equation relating the Jacobians on retrieval levels to the full-state Jacobian:

$$\frac{\partial \mathbf{L}}{\partial \boldsymbol{\gamma}} = \frac{\partial \mathbf{L}}{\partial \boldsymbol{x}} \frac{\partial \boldsymbol{x}}{\partial \beta} \frac{\partial \beta}{\partial \boldsymbol{\gamma}} \tag{A5}$$

or

$$\mathbf{K}_\gamma = \mathbf{K}_x \mathbf{M}_x \mathbf{M} = \mathbf{K}_\beta \mathbf{M}. \tag{A6}$$

If the estimated state is "close" to the true state, then the estimated state for a single measurement can be expressed as a linear retrieval equation (Rodgers, 2000):

$$\hat{\beta} = \beta_a + \mathbf{A}_\beta (\beta - \beta_a) + \mathbf{M}\mathbf{G}_\gamma \boldsymbol{\varepsilon}_n + \sum_l \mathbf{M}\mathbf{G}_\gamma \mathbf{K}_b^l \Delta b^l \tag{A7}$$

where $\boldsymbol{\varepsilon}_n$ is a zero-mean noise vector with covariance $\mathbf{S}_e$ and the vector Δb^l is the error in true state of parameters (l) that also affect the modeled radiance, e.g., temperature, interfering gases, spectroscopy. The $\mathbf{K}_b^l$ is the Jacobian of parameter (l). In this study, we found the systematic error is primarily due to the temperature uncertainty ($\boldsymbol{\varepsilon}_T$) and spectroscopic error ($\boldsymbol{\varepsilon}_L$). $\mathbf{G}_\gamma$ is the gain matrix, which is defined by

$$\mathbf{G}_\gamma = \frac{\partial \boldsymbol{\gamma}}{\partial \mathbf{L}} = \left(\mathbf{K}_\gamma^T \mathbf{S}_e^{-1} \mathbf{K}_\gamma + \mathbf{S}_a^{-1} \right)^{-1} \mathbf{K}_\gamma^T \mathbf{S}_e^{-1}. \tag{A8}$$

The averaging kernel for β in forward model dimension is

$$\mathbf{A}_\beta = \mathbf{M}\mathbf{G}_\gamma \mathbf{K}_\beta. \tag{A9}$$

We can define $\mathbf{A}_x = \mathbf{M}_x \mathbf{A}_\beta \mathbf{M}_x^{-1}$ as the averaging kernel for the concentration profile $\boldsymbol{x}$. In order to convert Eq. (A7) to the state vector of concentration ($\hat{\boldsymbol{x}}$), we apply Eq. (A7) into Eq. (A3):

$$\hat{\boldsymbol{x}} = \boldsymbol{x}_a + \mathbf{A}_x (\boldsymbol{x} - \boldsymbol{x}_a) + \mathbf{M}_x \mathbf{M}\mathbf{G}_\gamma \boldsymbol{\varepsilon}_n$$
$$+ \mathbf{M}_x \mathbf{M}\mathbf{G}_\gamma \mathbf{K}_T \boldsymbol{\varepsilon}_T + \mathbf{M}_x \mathbf{M}\mathbf{G}_\gamma \mathbf{K}_L \boldsymbol{\varepsilon}_L. \tag{A10}$$

The temperature uncertainty ($\boldsymbol{\varepsilon}_T$) and spectroscopic error ($\boldsymbol{\varepsilon}_L$) represent the systematic errors (Δb^l).

A2 Total error budget

The total error for a single retrieval is the difference between the estimated state vector (Eq. A10) and the true state vector ($\boldsymbol{x}$):

$$\delta\hat{\boldsymbol{x}} = \hat{\boldsymbol{x}} - \boldsymbol{x} = (\mathbf{I} - \mathbf{A}_x)(\boldsymbol{x}_a - \boldsymbol{x}) + \mathbf{M}_x \mathbf{M}\mathbf{G}_\gamma \boldsymbol{\varepsilon}_n$$
$$+ \mathbf{M}_x \mathbf{M}\mathbf{G}_\gamma \mathbf{K}_T \boldsymbol{\varepsilon}_T + \mathbf{M}_x \mathbf{M}\mathbf{G}_\gamma \mathbf{K}_L \boldsymbol{\varepsilon}_L. \tag{A11}$$

The second-order statistics for the error is

$$\mathbf{S}_{\delta\hat{x}} = \hat{\mathbf{S}}_{\text{sm}} + \hat{\mathbf{S}}_m + \hat{\mathbf{S}}_T + \hat{\mathbf{S}}_L \qquad (A12)$$

where the smoothing error covariance is

$$\hat{\mathbf{S}}_{\text{sm}} = (\mathbf{I} - \mathbf{A}_x)\,\mathbf{S}_a\,(\mathbf{I} - \mathbf{A}_x)^T\,; \qquad (A13)$$

a measurement error covariance is

$$\hat{\mathbf{S}}_m = \mathbf{M}_x\,\mathbf{MG}\mathbf{S}_e\,(\mathbf{M}_x\,\mathbf{MG})^T\,, \qquad (A14)$$

and two systematic error covariance matrices are

$$\hat{\mathbf{S}}_T = \mathbf{M}_x\,\mathbf{MG}\mathbf{K}_T\,\mathbf{S}_T\,(\mathbf{M}_x\,\mathbf{MG}\mathbf{K}_T)^T \qquad (A15)$$
$$\hat{\mathbf{S}}_L = \mathbf{M}_x\,\mathbf{MG}\mathbf{K}_L\,\mathbf{S}_L\,(\mathbf{M}_x\,\mathbf{MG}\mathbf{K}_L)^T\,. \qquad (A16)$$

$\mathbf{S}_a$ is the a priori covariance for CO_2, $\mathbf{S}_e$ the covariance describing the TCCON measurement noise (see Sect. 4), $\mathbf{S}_T$ the a priori covariance for temperature and based on the a priori covariance used for the Aura TES temperature retrievals (Worden et al., 2004); this temperature covariance is based on the expected uncertainty in the re-analysis fields that are inputs to the TES retrievals. $\mathbf{S}_L$ is the covariance associated with spectroscopic error. It has been found that spectroscopic inadequacies are common to all retrievals from TCCON radiances (e.g., line widths, neglect of line-mixing, inconsistencies in the relative strengths of weak and strong lines) (Wunch et al., 2010).

A3 Individual error budget terms

Considering different time scales, the uncertainties of the estimates would be attributed to different error terms. In this section, we will discuss the error terms one by one.

For comparisons of TCCON retrievals to each aircraft profile, we choose the TCCON measurements taken within a 4-h time window centered about the aircraft measurement. This time window is short enough so that we can assume the atmospheric state has not changed, but it is also long enough that there are enough samples of retrievals for good statistics (e.g., ~ 100 samples).

There are 41 aircraft measurements that measured CO_2 profiles over Lamont in 2009. On any given day (or i-th day), we have n_i TCCON retrievals within a 4-h time window around aircraft measurement where n_i varies by day (or aircraft profile comparison). The difference of the mean of these retrievals to the aircraft measurement can be used to compute the error of the mean estimate due to temperature. The average of the errors from these 41 comparisons estimates the mean bias error. Which term contributes to the uncertainties will be discussed in follow.

A3.1 Error due to extrapolation of CO_2 above aircraft profile

In reality, the true state (x) is unknown and can only be estimated by our best measurements, such as by aircraft, which

have a precision of 0.02 ppm. With the validation standard, the error in the retrieval ($\delta\hat{x}$) can be estimated by the comparison of the retrieved state vector ($\hat{x}$) to the validation standard ($\hat{x}_{\text{std}}$). In order to do an inter-comparison of the measurements from two different instruments, we apply a smoothing operator described in Rodgers and Connor (2003) to the complete profile (x_{FLT}) based on aircraft measurement so that it is smoothed by the averaging kernel and a priori constraint from the TCCON profile retrieval:

$$\hat{x}_{\text{std}} = x_a + \mathbf{A}_x\,(x_{\text{FLT}} - x_a). \qquad (A17)$$

$\hat{x}_{\text{std}}$ is the profile that would be retrieved from TCCON measurements for the same air sampled by the aircraft without the presence of other errors. x_{FLT} is the complete CO_2 profile based on aircraft measurement.

Several aircraft only measure CO_2 up to approximately 6 km, but three of them go up to 10 km or higher, which are measured by Learjet on 31 July, 2 and 3 August (Fig. 5). These three profiles show that the free troposphere is well mixed and the vertical gradient is small (Wofsy et al., 2011), less than $1\,\text{ppm km}^{-1}$ on average between 600 hPa and tropopause. Therefore, the lower part of $\mathbf{x_{FLT}}$ is from the direct aircraft measurements. Above that, the TCCON prior is scaled to the measured CO_2 values at the top of the aircraft measurement so that the profile is continuously extended up to 71 km. Then the complete profile based on the aircraft measurement is

$$x_{\text{FLT}} = \begin{bmatrix} x_{\text{FLT}}^{\text{meas}} \\ \lambda x_a^F \end{bmatrix} = x - \delta x_{\text{FLT}} = x - \begin{bmatrix} \delta x_{\text{FLT}}^{\text{meas}} \\ x^F - \lambda x_a^F \end{bmatrix} \quad (A18)$$

where $x_{\text{FLT}}^{\text{meas}}$ is the direct aircraft measurements in the lower atmosphere, which has been mapped to forward model grid. $\delta x_{\text{FLT}}^{\text{meas}}$ is its unknown error relative to the "truth" and is of the order of 0.02 ppm. λ is the ratio between the CO_2 at the top of aircraft measurement to the a priori CO_2 on that level. x_a^F and x^F represent the a priori and "true" state above direct aircraft measurement in the free troposphere and above. λx_a^F is the shifted a priori to smoothly extend the profile up to the stratosphere. x_{FLT} represents the complete profile based combining a priori. δx_{FLT} is the unknown error in the x_{FLT} to the true state.

Subtracting Eq. (A27) from Eq. (A10) results in the following expression:

$$\delta\hat{x} = \hat{x} - \hat{x}_{\text{std}} = \mathbf{A}_x\,\delta x_{\text{FLT}} + \mathbf{M}_x\,\mathbf{MG}_\gamma\,\boldsymbol{\varepsilon}_n$$
$$+ \mathbf{M}_x\,\mathbf{MG}_\gamma\,\mathbf{K}_T\,\boldsymbol{\varepsilon}_T + \mathbf{M}_x\,\mathbf{MG}_\gamma\,\mathbf{K}_L\,\boldsymbol{\varepsilon}_L. \qquad (A19)$$

The second-order statistics for the error in the complete aircraft-based profile, δx_{FLT}, is:

$$\mathbf{S}_{\delta x_{\text{FLT}}} = \mathbf{E}\,[\delta x_{\text{FLT}} - \mathbf{E}\,(\delta x_{\text{FLT}})]\,[x_{\text{FLT}} - \mathbf{E}\,(\delta x_{\text{FLT}})]^T$$
$$= \begin{bmatrix} \mathbf{S}_{\text{FLT}}^{\text{meas}} & \mathbf{0} \\ \mathbf{0} & \mathbf{S}_a^F \end{bmatrix}. \qquad (A20)$$

$\mathbf{S}_{\text{FLT}}^{\text{meas}}$ is the error covariance for direct aircraft measurements, which is a diagonal matrix with a constant value of the square

of 0.02 ppm (the precision of aircraft instruments) (Wunch et al., 2010). $\mathbf{S}_a^F$ is the submatrix of TCCON prior covariance matrix above the aircraft measurements. Since we scale the a priori to the aircraft data, the actual error covariance in the upper atmosphere should be much smaller than $\mathbf{S}_a^F$.

The uncertainty in retrieved column averages driven by the smoothing error can be estimated by

$$\sigma_{\rm sm}\left(\delta X_{\rm CO_2}\right) = \sqrt{h^T \mathbf{A}_x \mathbf{S}_\delta \, \boldsymbol{x}_{\rm FLT} \mathbf{A}_x^T \, h}. \tag{A21}$$

The upper limit of this uncertainty is approximately 0.5 ppm when using the a priori covariance in the upper atmosphere where the aircraft measurement is missing (e.g., above 6 km). Since the free troposphere is well mixed and the upper atmosphere is constrained by the aircraft measurement, the actual uncertainty for the validation standard should be much smaller than above estimates. For example, if we assume conservatively that the term $\mathbf{S}_{\delta x_{\rm FLT}}$ is half the size of the $\mathbf{S}_a$ used to describe our CO$_2$ covariance, then this term becomes negligible relative to the temperature error.

A3.2 Measurement error

The measurement noise vector $\boldsymbol{\varepsilon}_{\rm n}$ is a zero-mean random variable. In a 4-h time window, the measurement error covariance will drive the variability of the retrieved column averages. The uncertainty in retrieved column averages driven by the measurement error can be estimated by

$$\sigma_m\left(\delta X_{\rm CO_2}\right) = \sqrt{h^T \hat{\mathbf{S}}_m \, h} \tag{A22}$$

where $\hat{\mathbf{S}}_m$ is defined in Eq. (A14). We calculate that this term is approximately 0.32 ppm. The error on the mean is related to the number of samples in 4-h time window:

$$\sigma_m\left(\delta X_{\rm CO_2}\right) = \sqrt{\frac{h^T \hat{\mathbf{S}}_m \, h}{n_i}} \tag{A23}$$

where n_i is number of retrieval samples within 4-h on i-th day (listed in Table 2).

A3.3 Temperature error

Within a 4-h time window, we assume that variations in temperature do not result in variations in the CO$_2$ estimate; however, the uncertainty in the temperature profiles will result in a bias:

$$\overline{\left(\delta X_{\rm CO_2}\right)_{T_i}} = h^T \mathbf{M}_x \mathbf{M} \mathbf{G}_\gamma \mathbf{K}_T \, \boldsymbol{\varepsilon}_{T_i}. \tag{A24}$$

However, $\boldsymbol{\varepsilon}_{T_i}$ varies from day to day. The mean bias error from temperature uncertainties over days becomes

$$\overline{\left(\delta X_{\rm CO_2}\right)_T} = h^T \mathbf{M}_x \mathbf{M} \mathbf{G}_\gamma \mathbf{K}_T \left(\frac{1}{m} \sum_{i=1}^{m} \boldsymbol{\varepsilon}_{T_i}\right) \tag{A25}$$

with a covariance of

$$\sigma_T\left(\delta X_{\rm CO_2}\right) = \sqrt{h^T \hat{\mathbf{S}}_T \, h} \tag{A26}$$

where $\hat{\mathbf{S}}_T$ is from Eq. (A25). The estimate of this term is, on average, approximately 0.69 ppm.

A3.4 Spectroscopic error

The spectroscopic error is another significant source of systematic error. Different from temperature error, it does not vary significantly on any time scales or even over different sites (Wunch et al., 2010). Therefore, its covariance is always negligible. However, it is found to be the primary source of the bias error.

$$\overline{\left(\delta X_{\rm CO_2}\right)_L} = h^T \mathbf{M}_x \mathbf{M} \mathbf{G}_\gamma \mathbf{K}_L \, \boldsymbol{\varepsilon}_L. \tag{A27}$$

The estimate of this term is about -5 ppm. It is mainly due to the error in O$_2$ cross section.

A4 Errors in LT column-averaged CO$_2$

We estimate the LT CO$_2$ by subtracting the TES assimilated free tropospheric CO$_2$ from the TCCON total column CO$_2$. The TCCON dry-air total column estimated by weighting the retrieved O$_2$ column has a bias of approximately -5.66 ppm. Therefore, we remove the bias using Eq. (9) before subtracting the free tropospheric partial column amount. Because the TCCON estimates and TES/GEOS-Chem estimates are independent estimates of CO$_2$, the uncertainties in the lower tropospheric estimates are simply the uncertainties summed in quadrature:

$$\sigma\left(\delta X_{\rm CO_2}^{LT}\right) = \sqrt{\sigma^2\left(\delta X_{\rm CO_2}^{\rm TES}\right) + \sigma^2\left(\delta X_{\rm CO_2}^{\rm TCCON}\right)}. \tag{A28}$$

The estimate of this term is 0.90 ppm. The TES assimilated free tropospheric bias error and uncertainty (0.38 ± 0.71 ppm) is estimated by the comparison to the free tropospheric estimates from the aircraft-based profile ($\boldsymbol{x}_{\rm FLT}$). The TCCON total column mean bias error and uncertainty (-5.66 ± 0.55 ppm) has been discussed in previous section.

References

Abshire, J. B., Riris, H., Allan, G. R., Weaver, C. J., Mao, J. P., Sun, X. L., Hasselbrack, W. E., Kawa, S. R., and Biraud, S.: Pulsed airborne lidar measurements of atmospheric CO_2 column absorption, Tellus B, 62, 770–783, doi:10.1111/j.1600-0889.2010.00502.x, 2010.

Baker, D. F., Bösch, H., Doney, S. C., O'Brien, D., and Schimel, D. S.: Carbon source/sink information provided by column CO_2 measurements from the Orbiting Carbon Observatory, Atmos. Chem. Phys., 10, 4145–4165, doi:10.5194/acp-10-4145-2010, 2010.

Beer, R., Glavich, T. A., and Rider, D. M.: Tropospheric emission spectrometer for the Earth Observing System's Aura Satellite, Appl. Optics, 40, 2356–2367, doi:10.1364/AO.40.002356, 2001.

Bey, I., Jacob, D. J., Yantosca, R. M., Logan, J. A., Field, B. D., Fiore, A. M., Li, Q. B., Liu, H. G. Y., Mickley, L. J., and Schultz, M. G.: Global modeling of tropospheric chemistry with assimilated meteorology: Model description and evaluation, J. Geophys. Res.-Atmos., 106, 23073–23095, doi:10.1029/2001JD000807, 2001.

Biraud, S. C., Torn, M. S., Smith, J. R., Sweeney, C., Riley, W. J., and Tans, P. P.: A multi-year record of airborne CO_2 observations in the US Southern Great Plains, Atmos. Meas. Tech. Discuss., 5, 7187–7222, doi:10.5194/amtd-5-7187-2012, 2012.

Bousquet, P., Peylin, P., Ciais, P., Le Quere, C., Friedlingstein, P., and Tans, P. P.: Regional changes in carbon dioxide fluxes of land and oceans since 1980, Science, 290, 1342–1346, doi:10.1126/science.290.5495.1342, 2000.

Bovensmann, H., Buchwitz, M., Burrows, J. P., Reuter, M., Krings, T., Gerilowski, K., Schneising, O., Heymann, J., Tretner, A., and Erzinger, J.: A remote sensing technique for global monitoring of power plant CO_2 emissions from space and related applications, Atmos. Meas. Tech., 3, 781–811, doi:10.5194/amt-3-781-2010, 2010.

Bowman, K. W., Rodgers, C. D., Kulawik, S. S., Worden, J., Sarkissian, E., Osterman, G., Steck, T., Lou, M., Eldering, A., Shephard, M., Worden, H., Lampel, M., Clough, S., Brown, P., Rinsland, C., Gunson, M., and Beer, R.: Tropospheric emission spectrometer: Retrieval method and error analysis, IEEE T. Geosci. Remote, 44, 1297–1307, doi:10.1109/TGRS.2006871234, 2006.

Brix, H., Menemenlis, D., Hill, C., Dutkiewicz, S., Jahn, O., Wang, D., Bowman, K., and Zhang, H.: Using Green's Functions to Initialize and adjust a Global, Eddying Ocean Biogeochemistry General Circulation Model, Ocean Model., submitted, 2012.

Chahine, M., Barnet, C., Olsen, E. T., Chen, L., and Maddy, E.: On the determination of atmospheric minor gases by the method of vanishing partial derivatives with application to CO_2, Geophys. Res. Lett., 32, L22803, doi:10.1029/2005GL024165, 2005.

Chevallier, F.: Impact of correlated observation errors on inverted CO_2 surface fluxes from OCO measurements, Geophys. Res. Lett., 34, L24804, doi:10.1029/2007GL030463, 2007.

Chevallier, F., Ciais, P., Conway, T. J., Aalto, T., Anderson, B. E., Bousquet, P., Brunke, E. G., Ciattaglia, L., Esaki, Y., Frohlich, M., Gomez, A., Gomez-Pelaez, A. J., Haszpra, L., Krummel, P. B., Langenfelds, R. L., Leuenberger, M., Machida, T., Maignan, F., Matsueda, H., Morgui, J. A., Mukai, H., Nakazawa, T., Peylin, P., Ramonet, M., Rivier, L., Sawa, Y., Schmidt, M., Steele, L. P., Vay, S. A., Vermeulen, A. T., Wofsy, S., and Worthy, D.: CO_2 surface fluxes at grid point scale estimated from a global 21 year reanalysis of atmospheric measurements, J. Geophys. Res.-Atmos., 115, D21307, doi:10.1029/2010jd013887, 2010.

Chevallier, F., Deutscher, N. M., Conway, T. J., Ciais, P., Ciattaglia, L., Dohe, S., Frohlich, M., Gomez-Pelaez, A. J., Griffith, D., Hase, F., Haszpra, L., Krummel, P., Kyro, E., Labuschagne, C., Langenfelds, R., Machida, T., Maignan, F., Matsueda, H., Morino, I., Notholt, J., Ramonet, M., Sawa, Y., Schmidt, M., Sherlock, V., Steele, P., Strong, K., Sussmann, R., Wennberg, P., Wofsy, S., Worthy, D., Wunch, D., and Zimnoch, M.: Global CO_2 fluxes inferred from surface air-sample measurements and from TCCON retrievals of the CO2 total column, Geophys. Res. Lett., 38, L24810, doi:10.1029/2011gl049899, 2011.

Christi, M. J. and Stephens, G. L.: Retrieving profiles of atmospheric CO_2 in clear sky and in the presence of thin cloud using spectroscopy from the near and thermal infrared: A preliminary case study, J. Geophys. Res.-Atmos., 109, D04316, doi:10.1029/2003JD004058, 2004.

Crisp, D., Atlas, R. M., Breon, F. M., Brown, L. R., Burrows, J. P., Ciais, P., Connor, B. J., Doney, S. C., Fung, I. Y., Jacob, D. J., Miller, C. E., O'Brien, D., Pawson, S., Randerson, J. T., Rayner, P., Salawitch, R. J., Sander, S. P., Sen, B., Stephens, G. L., Tans, P. P., Toon, G. C., Wennberg, P. O., Wofsy, S. C., Yung, Y. L., Kuang, Z. M., Chudasama, B., Sprague, G., Weiss, B., Pollock, R., Kenyon, D., and Schroll, S.: The orbiting carbon observatory (OCO) mission, Adv. Space Res., 34, 700–709, doi:10.1016/j.asr.2003.08.062, 2004.

Crisp, D., Fisher, B. M., O'Dell, C., Frankenberg, C., Basilio, R., Bösch, H., Brown, L. R., Castano, R., Connor, B., Deutscher, N. M., Eldering, A., Griffith, D., Gunson, M., Kuze, A., Mandrake, L., McDuffie, J., Messerschmidt, J., Miller, C. E., Morino, I., Natraj, V., Notholt, J., O'Brien, D. M., Oyafuso, F., Polonsky, I., Robinson, J., Salawitch, R., Sherlock, V., Smyth, M., Suto, H., Taylor, T. E., Thompson, D. R., Wennberg, P. O., Wunch, D., and Yung, Y. L.: The ACOS CO_2 retrieval algorithm – Part II: Global X_{CO_2} data characterization, Atmos. Meas. Tech., 5, 687–707, doi:10.5194/amt-5-687-2012, 2012.

Deutscher, N. M., Griffith, D. W. T., Bryant, G. W., Wennberg, P. O., Toon, G. C., Washenfelder, R. A., Keppel-Aleks, G., Wunch, D., Yavin, Y., Allen, N. T., Blavier, J.-F., Jiménez, R., Daube, B. C., Bright, A. V., Matross, D. M., Wofsy, S. C., and Park, S.: Total column CO_2 measurements at Darwin, Australia – site description and calibration against in situ aircraft profiles, Atmos. Meas. Tech., 3, 947–958, doi:10.5194/amt-3-947-2010, 2010.

Fu, D., Worden, J. R., Liu, X., Kulawik, S. S., Bowman, K. W., and Natraj, V.: Characterization of ozone profiles derived from Aura TES and OMI Radiances, Atmos. Chem. Phys. Discuss., 12, 27589–27636, doi:10.5194/acpd-12-27589-2012, 2012.

Geibel, M. C., Gerbig, C., and Feist, D. G.: A new fully automated FTIR system for total column measurements of greenhouse gases, Atmos. Meas. Tech., 3, 1363–1375, doi:10.5194/amt-3-1363-2010, 2010.

Gurney, K. R., Law, R. M., Denning, A. S., Rayner, P. J., Baker, D., Bousquet, P., Bruhwiler, L., Chen, Y. H., Ciais, P., Fan, S., Fung, I. Y., Gloor, M., Heimann, M., Higuchi, K., John, J., Maki, T., Maksyutov, S., Masarie, K., Peylin, P., Prather, M., Pak, B. C., Randerson, J., Sarmiento, J., Taguchi, S., Takahashi, T., and Yuen, C. W.: Towards robust regional estimates of CO_2 sources and sinks using atmospheric transport models, Nature, 415, 626–630, doi:10.1038/415626a, 2002.

Henze, D. K., Hakami, A., and Seinfeld, J. H.: Development of the adjoint of GEOS-Chem, Atmos. Chem. Phys., 7, 2413–2433, doi:10.5194/acp-7-2413-2007, 2007.

Henze, D. K., Seinfeld, J. H., and Shindell, D. T.: Inverse modeling and mapping US air quality influences of inorganic $PM_{2.5}$ precursor emissions using the adjoint of GEOS-Chem, Atmos. Chem. Phys., 9, 5877–5903, doi:10.5194/acp-9-5877-2009, 2009.

Keppel-Aleks, G., Wennberg, P. O., and Schneider, T.: Sources of variations in total column carbon dioxide, Atmos. Chem. Phys., 11, 3581–3593, doi:10.5194/acp-11-3581-2011, 2011.

Keppel-Aleks, G., Wennberg, P. O., Washenfelder, R. A., Wunch, D., Schneider, T., Toon, G. C., Andres, R. J., Blavier, J.-F., Connor, B., Davis, K. J., Desai, A. R., Messerschmidt, J., Notholt, J., Roehl, C. M., Sherlock, V., Stephens, B. B., Vay, S. A., and Wofsy, S. C.: The imprint of surface fluxes and transport on variations in total column carbon dioxide, Biogeosciences, 9, 875–891, doi:10.5194/bg-9-875-2012, 2012.

Kopacz, M., Jacob, D. J., Henze, D. K., Heald, C. L., Streets, D. G., and Zhang, Q.: Comparison of adjoint and analytical Bayesian inversion methods for constraining Asian sources of carbon monoxide using satellite (MOPITT) measurements of CO columns, J. Geophys. Res.-Atmos., 114, D04305, doi:10.1029/2007JD009264, 2009.

Kuai, L., Wunch, D., Shia, R. L., Connor, B., Miller, C., and Yung, Y.: Vertically constrained CO_2 retrievals from TCCON measurements, J. Quant. Spectrosc. Ra., 113, 1753–1761, doi:10.1016/j.jqsrt.2012.04.024, 2012.

Kulawik, S. S., Jones, D. B. A., Nassar, R., Irion, F. W., Worden, J. R., Bowman, K. W., Machida, T., Matsueda, H., Sawa, Y., Biraud, S. C., Fischer, M. L., and Jacobson, A. R.: Characterization of Tropospheric Emission Spectrometer (TES) CO_2 for carbon cycle science, Atmos. Chem. Phys., 10, 5601–5623, doi:10.5194/acp-10-5601-2010, 2010.

Kulawik, S. S., Worden, J. R., Wofsy, S. C., Biraud, S. C., Nassar, R., Jones, D. B. A., Olsen, E. T., and Osterman, and the TES and HIPPO teams, G. B.: Comparison of improved Aura Tropospheric Emission Spectrometer (TES) CO_2 with HIPPO and SGP aircraft profile measurements, Atmos. Chem. Phys. Discuss., 12, 6283–6329, doi:10.5194/acpd-12-6283-2012, 2012.

Law, R. M. and Rayner, P. J.: Impacts of seasonal covariance on CO_2 inversions, Global Biogeochem. Cy., 13, 845–856, doi:10.1029/1999GB900073, 1999.

Messerschmidt, J., Geibel, M. C., Blumenstock, T., Chen, H., Deutscher, N. M., Engel, A., Feist, D. G., Gerbig, C., Gisi, M., Hase, F., Katrynski, K., Kolle, O., Lavric, J. V., Notholt, J., Palm, M., Ramonet, M., Rettinger, M., Schmidt, M., Sussmann, R., Toon, G. C., Truong, F., Warneke, T., Wennberg, P. O., Wunch, D., and Xueref-Remy, I.: Calibration of TCCON column-averaged CO_2: the first aircraft campaign over European TCCON sites, Atmos. Chem. Phys., 11, 10765–10777, doi:10.5194/acp-11-10765-2011, 2011.

Nassar, R., Jones, D. B. A., Suntharalingam, P., Chen, J. M., Andres, R. J., Wecht, K. J., Yantosca, R. M., Kulawik, S. S., Bowman, K. W., Worden, J. R., Machida, T., and Matsueda, H.: Modeling global atmospheric CO_2 with improved emission inventories and CO_2 production from the oxidation of other carbon species, Geosci. Model Dev., 3, 689–716, doi:10.5194/gmd-3-689-2010, 2010.

Nassar, R., Jones, D. B. A., Kulawik, S. S., Worden, J. R., Bowman, K. W., Andres, R. J., Suntharalingam, P., Chen, J. M., Brenninkmeijer, C. A. M., Schuck, T. J., Conway, T. J., and Worthy, D. E.: Inverse modeling of CO_2 sources and sinks using satellite observations of CO_2 from TES and surface flask measurements, Atmos. Chem. Phys., 11, 6029–6047, doi:10.5194/acp-11-6029-2011, 2011.

O'Brien, D. M. and Rayner, P. J.: Global observations of the carbon budget: 2. CO_2 column from differential absorption of reflected sunlight in the 1.61 μm band of CO_2, J. Geophys. Res.-Atmos., 107, 4354, doi:10.1029/2001JD000617, 2002.

O'Dell, C. W., Day, J. O., Pollock, R., Bruegge, C. J., O'Brien, D. M., Castano, R., Tkatcheva, I., Miller, C. E., and Crisp, D.: Preflight Radiometric Calibration of the Orbiting Carbon Observatory, IEEE T. Geosci. Remote, 49, 2438–2447, doi:10.1109/TGRS.2010.2090887, 2011.

O'Dell, C. W., Connor, B., Bösch, H., O'Brien, D., Frankenberg, C., Castano, R., Christi, M., Eldering, D., Fisher, B., Gunson, M., McDuffie, J., Miller, C. E., Natraj, V., Oyafuso, F., Polonsky, I., Smyth, M., Taylor, T., Toon, G. C., Wennberg, P. O., and Wunch, D.: The ACOS CO_2 retrieval algorithm – Part 1: Description and validation against synthetic observations, Atmos. Meas. Tech., 5, 99–121, doi:10.5194/amt-5-99-2012, 2012.

Parrington, M., Palmer, P. I., Henze, D. K., Tarasick, D. W., Hyer, E. J., Owen, R. C., Helmig, D., Clerbaux, C., Bowman, K. W., Deeter, M. N., Barratt, E. M., Coheur, P.-F., Hurtmans, D., Jiang, Z., George, M., and Worden, J. R.: The influence of boreal biomass burning emissions on the distribution of tropospheric ozone over North America and the North Atlantic during 2010, Atmos. Chem. Phys., 12, 2077–2098, doi:10.5194/acp-12-2077-2012, 2012.

Rayner, P. J. and O'Brien, D. M.: The utility of remotely sensed CO_2 concentration data in surface source inversions, Geophys. Res. Lett., 28, 175, doi:10.1029/2000GL011912, 2001.

Rayner, P. J., Law, R. M., Allison, C. E., Francey, R. J., Trudinger, C. M., and Pickett-Heaps, C.: Interannual variability of the global carbon cycle (1992–2005) inferred by inversion of atmospheric CO_2 and $\Delta^{13}CO_2$ measurements, Global Biogeochem. Cy., 22, GB3008, doi:10.1029/2007GB003068, 2008.

Rayner, P. J., Koffi, E., Scholze, M., Kaminski, T., and Dufresne, J. L.: Constraining predictions of the carbon cycle using data, Philos. T. Roy. Soc. A, 369, 1955–1966, doi:10.1098/rsta.2010.0378, 2011.

Rodgers, C. D.: Inverse Methods for Atmospheric Sounding: Theory and Practice, World Scientific, London, 256 pp., 2000.

Rodgers, C. D. and Connor, B. J.: Intercomparison of remote sounding instruments, J. Geophys. Res.-Atmos., 108, 4116, doi:10.1029/2002JD002299, 2003.

Sarrat, C., Noilhan, J., Lacarrere, P., Donier, S., Lac, C., Calvet, J. C., Dolman, A. J., Gerbig, C., Neininger, B., Ciais, P., Paris, J. D., Boumard, F., Ramonet, M., and Butet, A.: Atmospheric CO$_2$ modeling at the regional scale: Application to the CarboEurope Regional Experiment, J. Geophys. Res.-Atmos., 112, D12105, doi:10.1029/2006JD008107, 2007.

Schneising, O., Buchwitz, M., Reuter, M., Heymann, J., Bovensmann, H., and Burrows, J. P.: Long-term analysis of carbon dioxide and methane column-averaged mole fractions retrieved from SCIAMACHY, Atmos. Chem. Phys., 11, 2863–2880, doi:10.5194/acp-11-2863-2011, 2011.

Schneising, O., Bergamaschi, P., Bovensmann, H., Buchwitz, M., Burrows, J. P., Deutscher, N. M., Griffith, D. W. T., Heymann, J., Macatangay, R., Messerschmidt, J., Notholt, J., Rettinger, M., Reuter, M., Sussmann, R., Velazco, V. A., Warneke, T., Wennberg, P. O., and Wunch, D.: Atmospheric greenhouse gases retrieved from SCIAMACHY: comparison to ground-based FTS measurements and model results, Atmos. Chem. Phys., 12, 1527–1540, doi:10.5194/acp-12-1527-2012, 2012.

Singh, K., Jardak, M., Sandu, A., Bowman, K., Lee, M., and Jones, D.: Construction of non-diagonal background error covariance matrices for global chemical data assimilation, Geosci. Model Dev., 4, 299–316, doi:10.5194/gmd-4-299-2011, 2011a.

Singh, K., Sandu, A., Bowman, K. W., Parrington, M., Jones, D. B. A., and Lee, M.: Ozone data assimilation with GEOS-Chem: a comparison between 3-D-Var, 4-D-Var, and suboptimal Kalman filter approaches, Atmos. Chem. Phys. Discuss., 11, 22247–22300, doi:10.5194/acpd-11-22247-2011, 2011b.

Stephens, B. B., Gurney, K. R., Tans, P. P., Sweeney, C., Peters, W., Bruhwiler, L., Ciais, P., Ramonet, M., Bousquet, P., Nakazawa, T., Aoki, S., Machida, T., Inoue, G., Vinnichenko, N., Lloyd, J., Jordan, A., Heimann, M., Shibistova, O., Langenfelds, R. L., Steele, L. P., Francey, R. J., and Denning, A. S.: Weak northern and strong tropical land carbon uptake from vertical profiles of atmospheric CO$_2$, Science, 316, 1732–1735, 10.1126/science.1137004, 2007.

Suntharalingam, P., Jacob, D. J., Palmer, P. I., Logan, J. A., Yantosca, R. M., Xiao, Y. P., Evans, M. J., Streets, D. G., Vay, S. L., and Sachse, G. W.: Improved quantification of Chinese carbon fluxes using CO$_2$/CO correlations in Asian outflow, J. Geophys. Res.-Atmos., 109, D18S18, 10.1029/2003JD004362, 2004.

Velazco, V. A., Buchwitz, M., Bovensmann, H., Reuter, M., Schneising, O., Heymann, J., Krings, T., Gerilowski, K., and Burrows, J. P.: Towards space based verification of CO$_2$ emissions from strong localized sources: fossil fuel power plant emissions as seen by a CarbonSat constellation, Atmos. Meas. Tech., 4, 2809–2822, doi:10.5194/amt-4-2809-2011, 2011.

von Engeln, A., Teixeira, J., Wickert, J., and Buehler, S. A.: Using CHAMP radio occultation data to determine the top altitude of the Planetary Boundary Layer, Geophys. Res. Lett., 32, L06815, doi:10.1029/2004GL022168, 2005.

Walker, T. W., Jones, D. B. A., Parrington, M., Henze, D. K., Murray, L. T., Bottenheim, J. W., Anlauf, K., Worden, J. R., Bowman, K. W., Shim, C., Singh, K., Kopacz, M., Tarasick, D. W., Davies, J., von der Gathen, P., Thompson, A. M., and Carouge, C. C.: Impacts of midlatitude precursor emissions and local photochemistry on ozone abundances in the Arctic, J. Geophys. Res.-Atmos., 117, D01305, doi:10.1029/2011JD016370, 2012.

Washenfelder, R. A., Toon, G. C., Blavier, J. F., Yang, Z., Allen, N. T., Wennberg, P. O., Vay, S. A., Matross, D. M., and Daube, B. C.: Carbon dioxide column abundances at the Wisconsin Tall Tower site, J. Geophys. Res.-Atmos., 111, D22305, doi:10.1029/2006JD007154, 2006.

Wofsy, S. C., Hippo Sci Team, Cooperating Modellers Team, and Satellite Team: HIAPER Pole-to-Pole Observations (HIPPO): fine-grained, global-scale measurements of climatically important atmospheric gases and aerosols, Philos. T. Roy. Soc. A, 369, 2073–2086, doi:10.1098/rsta.2010.0313, 2011.

Worden, H. M., Deeter, M. N., Edwards, D. P., Gille, J. C., Drummond, J. R., and Nedelec, P.: Observations of near-surface carbon monoxide from space using MOPITT multispectral retrievals, J. Geophys. Res.-Atmos., 115, D18314, doi:10.1029/2010JD014242, 2010.

Worden, J., Kulawik, S. S., Shephard, M. W., Clough, S. A., Worden, H., Bowman, K., and Goldman, A.: Predicted errors of tropospheric emission spectrometer nadir retrievals from spectral window selection, J. Geophys. Res.-Atmos., 109, D09308, doi:10.1029/2004JD004522, 2004.

Worden, J., Liu, X., Bowman, K., Chance, K., Beer, R., Eldering, A., Gunson, M., and Worden, H.: Improved tropospheric ozone profile retrievals using OMI and TES radiances, Geophys. Res. Lett., 34, L01809, doi:10.1029/2006GL027806, 2007.

Wu, S. L., Mickley, L. J., Jacob, D. J., Logan, J. A., Yantosca, R. M., and Rind, D.: Why are there large differences between models in global budgets of tropospheric ozone?, J. Geophys. Res.-Atmos., 112, D05302, doi:10.1029/2006JD007801, 2007.

Wunch, D., Toon, G. C., Wennberg, P. O., Wofsy, S. C., Stephens, B. B., Fischer, M. L., Uchino, O., Abshire, J. B., Bernath, P., Biraud, S. C., Blavier, J.-F. L., Boone, C., Bowman, K. P., Browell, E. V., Campos, T., Connor, B. J., Daube, B. C., Deutscher, N. M., Diao, M., Elkins, J. W., Gerbig, C., Gottlieb, E., Griffith, D. W. T., Hurst, D. F., Jiménez, R., Keppel-Aleks, G., Kort, E. A., Macatangay, R., Machida, T., Matsueda, H., Moore, F., Morino, I., Park, S., Robinson, J., Roehl, C. M., Sawa, Y., Sherlock, V., Sweeney, C., Tanaka, T., and Zondlo, M. A.: Calibration of the Total Carbon Column Observing Network using aircraft profile data, Atmos. Meas. Tech., 3, 1351–1362, doi:10.5194/amt-3-1351-2010, 2010.

Wunch, D., Toon, G. C., Blavier, J. F. L., Washenfelder, R. A., Notholt, J., Connor, B. J., Griffith, D. W. T., Sherlock, V., and Wennberg, P. O.: The Total Carbon Column Observing Network (TCCON), Philos. T. Roy. Soc. A, 369, 2087–2112, doi:10.1098/rsta.2010.0240, 2011a.

Wunch, D., Wennberg, P. O., Toon, G. C., Connor, B. J., Fisher, B., Osterman, G. B., Frankenberg, C., Mandrake, L., O'Dell, C., Ahonen, P., Biraud, S. C., Castano, R., Cressie, N., Crisp, D., Deutscher, N. M., Eldering, A., Fisher, M. L., Griffith, D. W. T., Gunson, M., Heikkinen, P., Keppel-Aleks, G., Kyrö, E., Lindenmaier, R., Macatangay, R., Mendonca, J., Messerschmidt, J., Miller, C. E., Morino, I., Notholt, J., Oyafuso, F. A., Rettinger, M., Robinson, J., Roehl, C. M., Salawitch, R. J., Sherlock, V., Strong, K., Sussmann, R., Tanaka, T., Thompson, D. R., Uchino, O., Warneke, T., and Wofsy, S. C.: A method for evaluating bias in global measurements of CO$_2$ total columns from space, Atmos. Chem. Phys., 11, 12317–12337, doi:10.5194/acp-11-12317-2011, 2011b.

Yang, Z. H., Toon, G. C., Margolis, J. S., and Wennberg, P. O.: Atmospheric CO$_2$ retrieved from ground-based near IR solar spectra, Geophys. Res. Lett., 29, 1339, 10.1029/2001GL014537, 2002.

Yoshida, Y., Yokota, T., Eguchi, N., Ota, Y., Tanaka, T., Watanabe, H., and Maksyutov, S.: Global Concentrations of CO$_2$ and CH$_4$ Retrieved from GOSAT: First Preliminary Results, Sci. Online Lett. Atmos., 5, 160–163, doi:10.2151/sola.2009-041, 2009.

Zhang, L., Jacob, D. J., Kopacz, M., Henze, D. K., Singh, K., and Jaffe, D. A.: Intercontinental source attribution of ozone pollution at western US sites using an adjoint method, Geophys. Res. Lett., 36, L11810, doi:10.1029/2009GL037950, 2009.